1 *In situ* differentiation of iridophore crystallotypes underlies
2 zebrafish stripe patterning
3
4 Dvir Gur[#,1,2], Emily Bain[#,3], Kory Johnson[4], Andy J. Aman[3], Amalia Pasoili[1], Jessica D.
5 Flynn[5], Michael C. Allen[6], Dimitri D. Deheyn[6], Jennifer C. Lee[5], Jennifer Lippincott-
6 Schwartz[*,1], David Parichy[*,3]
7
8 [1] HHMI Janelia Research Campus, Ashburn, VA
9 [2] National Institute of Child Health and Human Development, NIH, Bethesda, MD
10 [3] Department of Biology and Department of Cell Biology, University of Virginia,
11   Charlottesville VA
12 [4] Bioinformatics Section, National Institute of Neurological Disorder and Stroke, NIH,
13   Bethesda, MD
14 [5] National Heart, Lung and blood Institute of, NIH, Bethesda, MD
15 [6] Marine Biology Research Division, Scripps Institution of Oceanography, University of
16   California, San Diego, La Jolla, CA
17
18 [#] Co-first authors
19 [*] Co-Corresponding authors
20
21 Correspondence: lippincottschwartz@janelia.hhmi.org; dparichy@virginia.edu
22

23 **Skin color patterns are ubiquitous in nature, evolve rapidly, and impact social**
24 **behavior[1], predator avoidance[2], and protection from ultraviolet irradiation[3]. A**
25 **leading model system for vertebrate skin patterning is the zebrafish[4-7]; its**
26 **alternating blue stripes and yellow interstripes depend on guanine crystal-**
27 **containing cells called iridophores that reflect light. It was suggested that the**
28 **zebrafish's alternating color pattern arises from a single type of iridophore**
29 **migrating differentially to stripes and interstripes[7-9]. When we tracked iridophores,**
30 **however, we found they did not migrate between stripes and interstripes but**
31 **instead differentiated and proliferated in place based on their micro-environment.**
32 **RNA seq analysis further revealed stripe and interstripe iridophores had different**
33 **transcriptomic states, while cryogenic scanning electron microscopy and micro-**
34 **X-ray diffraction showed they had different guanine crystal organizations and**
35 **responsiveness to norepinephrine, all indicating that stripe and interstripe**
36 **iridophores are different cell types. Based on these results, we present a new**
37 **model of skin patterning in zebrafish in which distinct iridophore crystallotypes**
38 **containing specialized, physiologically responsive, subcellular organelles arise in**
39 **stripe and interstripe zones by *in situ* differentiation. In this model, pattern**
40 **phenotype depends not only on interactions among pigment cells that affect their**
41 **arrangements, but also on factors that specify subcellular organization and**
42 **physiological responsiveness of specialized organelles.**
43

1   **Introduction**

2   Biological patterning is ubiquitous in nature, but mechanisms underlying its
3   establishment and maintenance have been well-documented in only a few instances that
4   are unlikely to represent the full spectrum of pattern-forming systems[6,10]. Indeed,
5   patterning can arise in response to graded positional information or by self-organization
6   of interacting cells, and it can require alternative specification of cell-types from a
7   common progenitor or sorting-out of cells that are heterogeneous already. Elucidating
8   the mechanisms required to pattern cells in diverse tissues and organs is fundamental to
9   understanding development and how phenotypes evolve.
10   The alternating dark (blue) and light (yellow) pigmented stripe pattern of adult
11   zebrafish *Danio rerio* (**Fig. 1a)** is a useful model for dissecting patterning
12   mechanisms[4,5,7,11,12]. Cells within the dark stripes include black pigment-containing
13   melanophores; cells in the light stripes (known as "interstripes") include orange-pigment
14   containing xanthophores; and both dark stripes and light interstripes contain specialized
15   cells called iridophores[13,14]. Iridophores are the major players for skin pattern
16   establishment and reiteration in zebrafish. They behave as reflective cells, exhibiting
17   angular-dependent changes in hue—iridescence—owing to membrane-bound reflecting
18   platelets of crystalline guanine[14-16]. In the light interstripes, iridophores have a cuboidal
19   shape and form an epithelial-like mat, presenting a "dense" morphological arrangement
20   (**Fig.1b**, fluorescence panel). In the dark stripes, by contrast, iridophores are sparse in
21   number and stellate in shape, and are sometimes referred to as having a "loose"
22   morphology[8] (**Fig.1b,** fluorescence panel). The iridophore's importance in skin patterning
23   has been demonstrated in experiments showing that genetically or experimentally
24   induced deficiencies in iridophores cause pattern defects, including alterations in primary
25   stripe positioning and boundary formation, and also lead to reductions or losses of
26   secondary interstripes and stripes[17-21]. In addition, an evolutionary truncation in
27   iridophore development leads to an attenuated stripe pattern in the zebrafish relative *D.*
28   *nigrofasciatus*[22].
29   An elegant model explaining the iridophore's role in stripe and interstripe formation
30   links pattern establishment and reiteration to changes in iridophore morphology,
31   proliferation and migration[7-9] (**Fig. 1c**, left panel). Densely arranged iridophores are
32   proposed to first proliferate to fill the primary interstripe. Some of these cells then adopt
33   a loose shape and migrate out into the stripe zone where they continue to proliferate.
34   Subsequently, some loose iridophores reaggregate to adopt a dense morphology and
35   thereby initiate secondary interstripes. The iridophore shape transitions from dense-to-
36   loose and loose-to-dense are thought to resemble epithelial-to-mesenchymal transitions
37   (EMT) and mesenchymal-to-epithelial transitions (MET), respectively. Signals by
38   melanophores and xanthophores are proposed to determine the specific morphologies
39   adopted by iridophores. Consistent with this idea, quantitative models incorporating
40   proposed dynamic morphological changes of individual iridophores are able to produce
41   stripe patterning and robustness[23,24].
42   Key predictions of the above model, hereafter referred to as "morphogenetic
43   respecification", are that some interstripe iridophores undergo an EMT-like
44   transformation and migrate out from the interstripe zone, while presumably maintaining

1   attributes (e.g., reflecting platelet composition and optical properties) other than their
2   overall shape. In testing these predictions through a variety of approaches, we found
3   that individual iridophores did not migrate out from the interstripe into the stripe. Instead,
4   iridophores assumed a particular morphology at the time of their differentiation according
5   to the presence or absence of melanophores and this morphology remained fixed
6   thereafter. We also observed that interstripe and stripe iridophores exhibited distinct
7   organizations of guanine-reflecting platelets (i.e., crystal types) conferring intrinsic
8   differences in color, and that only stripe-localized iridophores could modulate reflecting-
9   platelet spacings physiologically (blue → yellow). Furthermore, interstripe and stripe
10   iridophores had distinct transcriptomic states. Based on these results, we propose a new
11   model for stripe pattern formation in the adult zebrafish in which iridophore precursor
12   cells undergo "differentiation *in situ*" into distinct iridophore types (i.e., crystallotypes)
13   (**Fig. 1c**, right panel). This process would depend on factors in the iridophore
14   environment that impact the specification and subcellular organization of specialized
15   organelles within iridophore-precursors.
16
17   **Results**

18   ***Time-lapse imaging reveals iridophores do not migrate out from the interstripe***

19   Stripe pattern establishment and reiteration in the zebrafish has been proposed to occur
20   through morphogenetic respecification, in which iridophores differentiate to form a
21   primary interstripe and then these cells or their progeny migrate out to contribute to
22   stripes as well as secondary interstripes and stripes[7-9,23] (**Fig. 1c**, left panel). Individual
23   cells would switch morphologies as appropriate to pattern context, undergoing
24   morphogenetic respecification via processes resembling EMT or MET.
25   To test this model, we examined iridophore behaviors by time-lapse imaging of
26   membrane targeted mCherry driven by regulatory elements of *pnp4a*[22,25]. If
27   morphogenetic respecification accounts for variation in iridophore morphology and
28   patterning, then events resembling EMT or MET should be observable: densely packed
29   iridophores of the completed interstripe should delaminate to populate the stripe,
30   whereas loosely arranged iridophores of completed stripes should aggregate to initiate
31   new interstripes. In over 300 hours of recordings, we observed no instances in which
32   interstripe iridophores—having the dense morphology—delaminated from their
33   neighbors and assumed the loose morphology (**Fig. 1d**; 14,475 total cells, including
34   1,637 cells located at interstripe edges). Likewise, interstripe iridophores that divided
35   yielded daughter cells that remained in the interstripe (981 divisions including 160 at
36   interstripe edges; **Fig. 1d**, **Extended Data Fig. 1a**, **Supplementary Movies S1**, **S2**).
37   These observations do not support the morphogenetic respecification model.
38   A different way to produce cells in distinct locations having distinct morphologies
39   would be if iridophores populate interstripes and stripes by differentiating from a
40   progenitor not yet specified to type (**Fig. 1c**, right panel). Iridophore morphology in this
41   model would emerge by "differentiation *in situ*" in response to context-appropriate
42   signals, and that same morphology would be retained thereafter by the cells or their
43   progeny. A prediction of this model for iridophore patterning is that new cells should

1　begin to express markers of iridophore differentiation during pattern formation.
2　Consistent with this hypothesis, we frequently observed cells acquire or increase
3　*pnp4a*:mem-mCherry expression within developing stripes (**Extended Data Figs. 1b-e**,
4　**Supplementary Movies S2–S5**).
5　　Quantitative image analyses of proliferation and migration further supported pattern
6　development by a mechanism of differentiation *in situ*. We found that proliferation of
7　loose iridophores within stripes was greater than dense iridophores within
8　interstripes[22](**Extended data Fig. 2a**). Moreover, iridophores within interstripes tended
9　to divide along an anterior–posterior plane, consistent with the known faster growth
10　along this axis than dorsoventrally[26] (**Extended Data Figs. 1b, 2b**). By contrast, planes
11　of division by stripe iridophores were more uniformly distributed, in keeping with a rapid
12　and relatively uniform occupancy of prospective stripe regions (**Extended data Figs. 1b-**
13　**e, 2b)**. Similarly, movements of dense iridophores were negligible, whereas loose
14　morphology iridophores could migrate up to several cell diameters and these
15　movements tended to be biased away from the first interstripe (**Extended Data Figs. 2c,**
16　**2d**, **Supplementary Movie S5**).

17　***Fate-mapping and repeated imaging support a model of differentiation in situ***

18　We next devised a further set of experiments to challenge the two models of iridophore
19　patterning by following the long-term fates of iridophores marked by photoconversion
20　(green → magenta) of nuclear-localizing *pnp4*:nucEos fluorescent protein. In this
21　experiment, photoconverted "old" iridophores will acquire white-colored nuclei over time
22　due to their having both newly synthesized nucEos[un] (unconverted green) and
23　photoconverted nucEos[conv] (magenta) in their nuclei; by contrast, "new" iridophores
24　formed from precursor cells will have only nucEos[un] (green) in their nuclei. (**Fig. 2a**)[27,28].
25　We reasoned that if individual iridophores change their morphological states and migrate
26　out to contribute to both interstripes and stripes, as predicted by the morphogenetic
27　respecification model, then marking cells in one pattern element should later yield
28　marked cells in both pattern elements. On the other hand, if individual iridophores are
29　fixed for their morphological state and contribute only to interstripes or stripes, as
30　predicted by the differentiation *in situ* model, marked cells should retain their morphology
31　and be confined to their original pattern element.
32　　Immediately after photoconverting a region in the interstripe zone, all iridophores in
33　this region had magenta nuclei, whereas iridophores in regions not targeted for
34　photoconversion, including a very few loose iridophores already present in the stripe
35　zone, had only green nuclei (**Figs. 2b,** post-photoconversion). After 7 days, only
36　iridophores in the interstripe zone had white nuclei, whereas newly-formed iridophores,
37　having green nuclei (indicative of their acquiring *pnp4* expression), could be seen mostly
38　in the stripe zone (**Figs. 2b,** After 7 day). The presence of white-colored nuclei in the
39　interstripe and their absence in the stripe clearly indicates that interstripe marked cells
40　did not migrate, favoring the model of differentiation *in situ*. Additionally, we found that
41　the formation of secondary interstripes was characterized by the development of cells
42　newly expressing *pnp4* within this region, suggesting differentiation with subsequent
43　proliferation rather than active aggregation (**Extended Data Fig. 3**).

4

1 The above analyses focused on a region in the middle of the flank. Because
2 iridophore behaviors may differ between anatomical regions, we extended our analyses
3 by examining distributions of *pnp4*:mem-mCherry+ cells in entire, individual fish imaged
4 daily over 33 d. These analyses also revealed extensive differentiation of iridophores
5 without indications of EMT (**Extended Data Figs. 4** and **5a,b Supplementary Movie**
6 **s6**). In some instances, patches of dense iridophores anteriorly appeared to split
7 between primary interstripe and ventral secondary interstripes, perhaps owing to rapid
8 expansion of the flank directly over the swim bladder (**Extended Data Fig. 5d**;
9 **Supplementary Movie S7**). In a minority of larvae (~20%), patches of 5–10 closely
10 associated iridophores developed anteriorly, dorsal to the primary interstripe. Cells in
11 these patches sometimes maintained their tight associations and became incorporated
12 into the secondary dorsal interstripe. In other instances, such cells were incorporated
13 instead into the stripe (**Extended Data Figs. 5c,e**). Contrary to the expectations of the
14 morphogenetic respecification model[8,23], the few of these cells that transitioned from a
15 nascent dense morphology to a loose morphology occurred already within prospective
16 stripe regions. These observations highlight subtle region-specific differences in
17 patterning events and suggest that, had state transitions occurred in a majority of cells or
18 over a broader anatomical area, as predicted in the morphological respecification model,
19 they should have been observed. That they were not observed lends further support to
20 the model of differentiation *in situ*.

21 ### *Role of melanophores in iridophore pattern remodeling*

22 Because melanophores reside in stripe- but not interstripe-zones, we wondered whether
23 iridophore pattern remodeling (i.e., dense- versus loose- arrangement morphology) is
24 impacted by melanophore presence. Prior work has hinted at this possibility as mutants
25 for melanophore-inducing trancription factor (*mitfa*), which lack melanophores, have the
26 dense-morphology iridophores (characteristic of interstripe zones) over a broader area
27 than in wild-type fish[18,29]. To explore this further, we used a temperature-sensitive allele,
28 *mitfa^{vc7}*, that allows conditional differentiation or ablation of melanophores[28,30,31] (**Fig.**
29 **2c**), and then examined the phenotypes of iridophores in different skin areas.
30 Cells in a defined area were marked by nucEos photoconversion and followed over
31 time after shifting between temperature regimes in order to assess whether iridophores
32 in newly arising stripes, or regions newly devoid of stripes, were derived either from
33 previously differentiated or newly differentiated cells. When fish were shifted from
34 restrictive temperature, where they lacked melanophores, to permissive temperature,
35 where melanophore differentiation could occur, we found that pre-existing, dense
36 morphology iridophores receded and new iridophores differentiated into a loose
37 arrangement in regions where melanophore differentiation had occurred (**Fig. 2d**;
38 **Extended Data Fig. 6a**). Reciprocal temperature shifts to ablate melanophores led to a
39 similar loss of pre-existing loose iridophores (through population turnover) and the
40 differentiation of new dense iridophores (**Extended Data Fig. 6b**). Though we cannot
41 exclude the possibility that some pre-existing iridophores were incorporated into
42 remodeled pattern elements, these results suggest that the presence of melanophores

1 has a major effect on the pattern remodeling of iridophores, specifically, in promoting a
2 loose morphology.

3 ***Distinct crystal morphology and ultrastructural organization but shared chemistry***
4 ***of loose and dense iridophores***

5 Differences in iridophore morphologies (dense/cuboidal vs loose/stellate) and our failure
6 to observe transitions between these two states, raised the possibility that iridophores of
7 dense/cuboidal morphology in interstripes and loose/stellate morphology in stripes
8 represent distinct cell subtypes, analogous to neuronal subtypes[32]. To test this
9 possibility, we evaluated the subcellular architecture, physiology and gene expression of
10 dense/cuboidal iridophores in stripes versus loose loose/stellate iridophores in
11 interstripes.
12   Because iridophores depend for their iridescence on stacks of membrane-bound
13 reflecting platelets consisting of crystalline guanine[5,16], we first asked whether numbers,
14 sizes or arrangements of these crystals differ between iridophores found in interstripe
15 versus stripe regions. To visualize guanine crystals *in situ* required a reagent that would
16 adhere to guanine crystals and so screened 12 cell-permeable dyes, chosen for their
17 ability to form both hydrogen bonds and pi-stacking interactions. We found that
18 Malachite Green efficiently bound guanine and therefore used it to examine guanine
19 crystal organization in iridophores from interstripe versus stripe regions. Incident
20 illumination images of the stripe zone showed blue, loosely distributed iridophores on top
21 of black melanophores, whereas images of the interstripe zone showed dense silvery
22 iridophores covered by yellow xanthophores (**Fig. 3a,b**, incident illumination). Notably,
23 Malachite Green labeling of guanine crystals within iridophores in these two zones
24 revealed tightly stacked arrays of crystals in loose iridophores from the stripe but
25 markedly disordered arrays of crystals in dense iridophores from the interstripe (**Fig. 3a-**
26 **b,** upper panels).
27   To assess ultrastructural organization of iridophores under near-physiological
28 conditions, in which crystal organization and cytoplasmic spacing are likely to be
29 retained, we used cryogenic scanning electron microscopy (cryo-SEM). Crystal arrays of
30 loose iridophores from stripes were remarkably ordered, with 20 to 30 layers of parallel
31 crystals having an average thickness of 27±7 nm (*n*=82), neatly separated by thin layers
32 of cytoplasm of average thickness 131±24 nm (*n*=91) (**Fig. 3a,** lower panel). By contrast,
33 crystal arrays of dense iridophores from interstripes were disordered, varying in both
34 orientations and spacings between crystals (**Fig. 3b,** lower panel), with 30–40 crystals
35 per cell, and a similar average crystal thickness of 25±8 nm (*n*=130) and an average
36 cytoplasm spacing of 186±81 (*n*=145).
37   Beyond differences in crystal arrangements, the shapes and sizes of crystals
38 appeared to differ between loose iridophores in stripes and dense iridophores in
39 interstripes. To quantify these differences, we isolated skin separately from stripes (**Fig.**
40 **3c**, left panel) and interstripes (**Fig. 3c,** right panel) and extracted crystals for
41 transmission electron microscopy (TEM) and electron diffraction (ED) analyses. While
42 the crystals in cells from both tissue regions comprised plates of β-guanine (**Fig. 3d**),
43 crystals isolated from stripe iridophores were smaller (3.9±0.4 µm vs. 5.3 ±0.9 µm) and

6

1 had smaller aspect ratios than crystals from interstripe iridophores (1.9±0.2 μm vs. 2.5
2 ±0.3 μm; n=57, 60) (**Fig. 3e**). *In situ* Raman spectroscopy of individual cells further
3 validated that crystals in loose iridophores in stripe zones and dense iridophores in
4 interstripe zones consist of β-guanine, and failed, within the accuracy afforded by these
5 measurements, to reveal other components, suggesting that differences in crystal
6 morphology are not related to their chemistry (**Extended Data Fig. 7**).

7 ### *Iridophore subtypes differ in their optical properties*

8 Differences in colors reflected by stripe iridophores (blue) and interstripe iridophores
9 (silvery-yellow) have sometimes been ascribed to influences of pigments contained
10 within melanophores and xanthophores, respectively. Given the differences we observed
11 in reflecting platelet architectures of iridophores from stripes versus interstripes,
12 however, we reasoned that reflected spectra might be intrinsic properties of iridophore
13 subtypes. Consistent with this hypothesis, we found close matches between spectra
14 predicted from simulations based on a Monte Carlo transfer matrix[33] (with morphometic
15 data derived from cryo-SEM) and empirical reflectance spectra recorded for individual
16 cells by hyperspectral imaging microscopy[34] (**Fig. 3f, g**). Indeed, simulations for ordered-
17 crystal iridophores from stripes predicted a peak in the blue region at 450 nm
18 approaching unity reflection, whereas simulations for disordered-crystal iridophores from
19 interstripes, predicted a broad wavelength reflection. In addition, while the reflection from
20 the ordered-crystal iridophores was highly dependent on the angle of incident light, the
21 reflection from disordered-crystal iridophores was not (**Extended Data Fig. 8)**.
22   We further found that intrinsic differences in iridophore optical properties could
23 generate a strong contrast in color between stripes and interstripes independent of
24 pigments in other cell types. This was manifested in fish that lack both melanin in
25 melanophores and carotenoids in xanthophores, owing to mutations in both *tyrosinase*
26 and *scarb1*, respectively[25]. Here, differences in color between stripes and interstripes
27 (i.e., blue versus silvery-yellow) persisted even in the absence of other pigments (**Fig.
28 3h**). Together, these results demonstrate the intrinsic differences in optical properties
29 between ordered-crystal iridophores of stripes and disordered-crystal iridophores from
30 interstripes.

31 ### *Disordered-crystal and ordered-crystal containing iridophores remain distinct
32 throughout development*

33 To map the structural organization of iridophores across the entire skin pattern, we used
34 synchrotron-based micro X-ray diffraction, which allows large areas to be scanned while
35 still providing information on orientations and anisotropy of crystal arrays at the level of a
36 single cell. In this system, high angular distribution diffractions having a full-ring signal
37 are indicative of crystal orientations that vary (i.e., disordered), whereas low angular
38 distribution diffractions having a punctuated-ring signal are indicative of crystals that are
39 consistently oriented (i.e., ordered*)*[15]. Dorso-ventral line scanning across the flank of the
40 fish demonstrated there were consistent differences in structural organization of stripe
41 vs. interstripe regions (**Fig. 4a**). Specifically, based on their (012) and (002) diffraction

1   planes[15,35], crystal plates in iridophores of the stripe zone were well oriented (i.e.,

2   ordered) (**Figs. 4a,** panels 1 and 3), whereas those in the interstripe zone were non-

3   aligned (i.e., disordered) (**Figs. 4a,** panels 2 and 4).

4   Our *mitfa[vc7]* photoconversion results (see **Fig. 2c**) raised the possibility that

5   melanophores promote the differentiation of progenitors into iridophores with ordered

6   crystal arrays. We tested this idea using micro X-ray diffraction to evaluate the crystals

7   architecture in iridophores of two zebrafish mutants: null-allele *mitfa[w2]* and *albino*. In

8   *mitfa[w2]* mutants, melanophores are missing owing to a defect in their specification; in

9   *albino* mutants, melanophores are present but lack melanin[29,36]. We reasoned that if

10   melanophores drive iridophore differentiation towards the ordered crystallotype, then

11   *mitfa[w2]* mutants should be deficient in iridophores having ordered crystals, whereas

12   *albino* mutants should retain ordered iridophores, similar to the wild type. Line scans

13   across the flanks of *mitfa[w2]* fish revealed mostly high angular distribution (012)

14   diffractions, typical of the disordered crystallotype (**Fig. 4b**). Scanning the entire fish,

15   showed some diffraction patterns corresponding to ordered iridophores, but these were

16   located towards the posterior and were a minor component of the diffractions (**Extended**

17   **Data Fig. 9**). The same analysis on *albino* fish revealed alternating diffraction patterns

18   similar to that seen in wild-type (**Fig. 4c**). These results suggest that melanophores

19   enhance the differentiation of ordered crystallotype iridophores.

20   We next examined the relative developmental timing of precursor differentiation into

21   disordered and ordered crystallotypes by assessing micro X-ray diffraction patterns over

22   ontogeny. In fish of 6.0 mm standardized standard length (SSL) and 6.5 SSL, which

23   have only a single interstripe and very few adult melanophores[26], we observed only

24   disordered crystallotype iridophores (having high angular distribution diffraction patterns

25   of the (012) plane) (**Fig. 4d**; **Extended Data Fig. 10**). When fish were ~6.9 SSL, with a

26   substantial complement of melanophores and loose iridophores, low angular distribution

27   diffraction patterns of the (002) plane, typical of ordered crystallotype iridophores,

28   became visible (**Fig. 4e**). These results supported the idea that precursor cells

29   differentiate into ordered crystallotype iridophores only after the differentiation of

30   disordered-crystallotype iridophores and in the presence of melanophores.

31   ***Ordered and disordered crystallotypes exhibit distinct transcriptomic signatures***

32

33   We next compared the transcriptomic signatures of ordered and disordered crystallotype

34   iridophores (i.e., from stripes and interstripes) by single cell RNA-sequencing (scRNA-

35   seq) (**Fig. 5a**). Dimensionality reduction followed by unsupervised clustering revealed six

36   clusters, three of which (clusters 4–6) contained cells expressing known markers of

37   iridophores[37] (i.e., *tfec, gpnmb*) (**Fig. 5b**). Expression of purine synthesis pathway

38   genes, markedly upregulated[25] in iridophores, further validated this initial assignment

39   (**Extended Data Fig. 11**). Next, we tested whether iridophore clusters recovered by

40   scRNA-seq corresponded to their anatomical sites of origin. Supporting this possibility,

41   98% of cells in cluster 5 originated from interstripes, and 85% of cells in cluster 4

42   originated from stripes (**Fig. 5c**). Cells of cluster 6 were split between interstripe (63%)

43   and stripe (37%) (**Extended Data Fig. 12**). Pseudotemporal ordering showed that

1   ordered-crystal iridophores and disordered-crystal iridophores were associated with
2   different branches in trajectories of inferred differentiation, whereas cluster 6 iridophores
3   spanned across branches (**Fig. 5d**). Several hundred loci were differentially expressed
4   between cells of clusters 4 and 5 (**Fig. 5e** and **Supporting information**), suggesting
5   candidate genes that may contribute to structural or other differences between stripe and
6   interstripe iridophores. We concluded from these analyses that iridophores of interstripe
7   and stripe zones are transcriptionally distinct.
8
9   *Physiological color change differs between iridophore subtypes*

10   Color pattern can be influenced physiologically[38,39], as some types of pigment cells
11   disperse or contract pigment granules in response to endocrine and neuroendocrine
12   factors, including norephinephrine (NE)[40-42]. We wondered whether differential
13   responses from the iridophore subtypes might contribute to this response. To test this,
14   we bathed isolated fish skin in 10 µM NE solution. Upon NE treatment, interstripe-
15   derived iridophores exhibited a ~120 nm shift in peak reflection, whereas stripe-derived
16   iridophores exhibited only a minor change in their overall organization of crystals and
17   spectrum of reflected light measured by hyperspectral imaging (**Fig. 5f**). Viewing the
18   response to NE in the context of the whole tissue also revealed a preferential color
19   change in striped- versus interstripe-zones (**Fig. 5g**). These results support prior work
20   showing that iridophores of different shapes respond differently to NE[40], and further
21   demonstrate that only stripe iridophores change their color upon NE treatment. This
22   differential response, in conjunction with the known aggregation of granules within
23   melanophores and xanthophores[41,42], could contribute to the dramatic reduction in
24   contrast between stripe and interstripe zones under NE treatment, which causes the
25   prominent zebrafish stripe pattern to diminish (**Supplementary movie 8**).

26   **Discussion**

27   Pigmentation of teleost fish has become a valuable system for understanding pattern
28   formation in animals, including how changes in pattern-forming mechanisms lead to
29   phenotypic variation within and between species[4,7,11]. In zebrafish, a widely accepted
30   model links dynamic changes in iridophore shape—between a dense morphology in
31   interstripes and a loose morphology in stripes—to establishment and reiteration of
32   pattern[8,9,23]. In this model, iridophores of interstripes and stripes are similar cells that
33   have merely adopted different morphologies as they migrate into different regions. Our
34   findings of substantial differences in ultrastructure, physiology and transcriptomic state of
35   iridophore subtypes—and the absence of morphological transitions predicted for
36   individual iridophores—support an alternative model of differentiation *in situ* for how the
37   reiterated stripe pattern of zebrafish develops. In this model, iridophore precursors in
38   developing stripes and interstripes differentiate *in situ* into distinct iridophore
39   crystallotypes with different subcellular organization and physiological responsiveness
40   based on their micro- environment.
41   Strongly supporting a model of differentiation *in situ* was our finding of substantial
42   physiological disparities between iridophores of stripes and interstripes. In particular,

1   iridophores of interstripes had larger reflecting crystal platelets that were disordered,
2   whereas those of stripes had smaller crystal platelets that were uniformly stacked and
3   oriented. The colors of these cells differed as well: iridophores in interstripes were
4   silvery-yellowish, and iridophores in stripes were blue, and these differences were
5   autonomous properties of the cells, not a consequence of pigments contained in other
6   pigment cells with which iridophores associate. Physiological responses also differed:
7   disordered crystal platelets of interstripe iridophores were refractory to NE, whereas,
8   ordered crystal platelets of stripe iridophores changed their cellular organization upon
9   NE treatment. Finally, iridophores from interstripes and stripes had distinct gene
10 expression profiles.

11   We found no evidence for another key prediction of the prior model, namely that
12 individual iridophores should undergo state transitions as cells originating in one pattern
13 element disperse to populate another. Photo-labeled iridophores observed over short or
14 long periods failed to migrate between interstripe and stripe zones, even when they were
15 challenged to undergo transitions in the context of pattern remodeling (stimulated by
16 changes in melanophore abundance). Instead, development and remodeling of
17 interstripes and stripes involved the *in situ* differentiation, subsequent proliferation, and
18 in some cases migration of iridophores with morphologies appropriate to their location
19 within the pattern. Only in a minority of fish, and in a small anatomical region, did we
20 observe patches of initially dense iridophores assume a loose arrangement. Such
21 behaviors occurred within prospective stripes, rather than at boundaries between
22 interstripes and stripes, as previously postulated, and involved cells that had not yet fully
23 differentiated.

24   These data all point to a model of stripe patterning that depends on differentiation *in*
25 *situ*. In this model, latent progenitors associated with the peripheral nervous system that
26 have transited to the skin during the larva-to-adult transformation expand clonally as
27 iridoblasts—not specified to subtype—and subsequently differentiate according to cues
28 in the microenvironment they encounter. Our data, together with those of others, suggest
29 that some of these signals depend on melanophores[18,19,27,43], promoting differentiation of
30 iridoblasts towards a state having ordered reflecting crystal platelets that are
31 physiologically responsive (blue ↔ yellow) in stripes, and away from an alternative state
32 of disordered crystal platelets lacking physiological responsiveness (silvery-yellow) in
33 interstripes. Additional signals from xanthophores, iridophores, and other cell types likely
34 contribute as well. Whether these events of specification unfold as iridoblasts expand
35 their territory within the plane of the skin hypodermis, or as they arrive at the hypodermis
36 after migrating from progenitor niches within the peripheral nervous system, remains to
37 be determined. Whichever mode of iridoblast morphogenesis holds true, our findings
38 highlight the importance of extrinsic factors that specify and promote the *in situ*
39 differentiation of iridophore subtypes during pattern establishment and reiteration. The
40 resulting iridophore subtypes likely allow the zebrafish to alter its skin patterning to make
41 it more or less distinctive, a trait crucial for the fish to be able to join shoals or obscure
42 itself[1,44].
43
44

Author contributions

Author contributions: D.G, E.J.B, D.D.D, J.C.L D.M.P., and J.L.-S. designed research; D.G, E.J.B, A.J.A, A.P, J.D.F, M.C.A, performed research; D.G, E.J.B, K.J, J.D.F, D.D.D, J.C.L D.M.P., and J.L.-S. analyzed data; and D.G, E.J.B, D.M.P., and J.L.-S. wrote the paper.

References

1   Rosenthal, G. G. & Ryan, M. J. Assortative preferences for stripes in danios. *Anim. Behav.* **70**, 1063-1066, doi:https://doi.org/10.1016/j.anbehav.2005.02.005 (2005).

2   Endler, J. A. in *Evolutionary Biology* (eds Max K. Hecht, William C. Steere, & Bruce Wallace) 319-364 (Springer US, 1978).

3   Kapp, F. G. *et al.* Protection from UV light is an evolutionarily conserved feature of the haematopoietic niche. *Nature* **558**, 445-448, doi:10.1038/s41586-018-0213-0 (2018).

4   Patterson, L. B. & Parichy, D. M. Zebrafish pigment pattern formation: insights into the development and evolution of adult form. *Annu. Rev. Genet.* **53**, 505-530, doi:10.1146/annurev-genet-112618-043741 (2019).

5   Schartl, M. *et al.* What is a vertebrate pigment cell? *Pigment Cell Melanoma Res.* **29**, 8-14, doi:10.1111/pcmr.12409 (2016).

6   Schweisguth, F. & Corson, F. Self-Organization in Pattern Formation. *Dev. Cell* **49**, 659-677, doi:10.1016/j.devcel.2019.05.019 (2019).

7   Irion, U., Singh, A. P. & Nusslein-Volhard, C. The Developmental Genetics of Vertebrate Color Pattern Formation: Lessons from Zebrafish. *Curr. Top. Dev. Biol.* **117**, 141-169, doi:10.1016/bs.ctdb.2015.12.012 (2016).

8   Singh, A. P., Schach, U. & Nusslein-Volhard, C. Proliferation, dispersal and patterned aggregation of iridophores in the skin prefigure striped colouration of zebrafish. *Nat. Cell. Biol.* **16**, 607-614, doi:10.1038/ncb2955 (2014).

9   Fadeev, A., Krauss, J., Frohnhofer, H. G., Irion, U. & Nusslein-Volhard, C. Tight Junction Protein 1a regulates pigment cell organisation during zebrafish colour patterning. *Elife* **4**, doi:10.7554/eLife.06545 (2015).

10   Dahmann, C., Oates, A. C. & Brand, M. Boundary formation and maintenance in tissue development. *Nat. Rev. Genet.* **12**, 43-55, doi:10.1038/nrg2902 (2011).

11   Kondo, S. & Watanabe, M. Black, yellow, or silver: which one leads skin pattern formation? *Pigment Cell Melanoma Res.* **28**, 2-4, doi:10.1111/pcmr.12328 (2015).

12   Eskova, A., Frohnhöfer, H. G., Nüsslein-Volhard, C. & Irion, U. Galanin Signaling in the Brain Regulates Color Pattern Formation in Zebrafish. *Curr. Biol.* **30**, 298-303., doi:https://doi.org/10.1016/j.cub.2019.11.033 (2020).

13   Hirata, M., Nakamura, K. & Kondo, S. Pigment cell distributions in different tissues of the zebrafish, with special reference to the striped pigment pattern. *Dev. Dyn.* **234**, 293-300, doi:10.1002/dvdy.20513 (2005).

14   Hirata, M., Nakamura, K., Kanemaru, T., Shibata, Y. & Kondo, S. Pigment cell organization in the hypodermis of zebrafish. *Dev. Dyn.* **227**, 497-503, doi:10.1002/dvdy.10334 (2003).

15   Gur, D. *et al.* The Dual Functional Reflecting Iris of the Zebrafish. *Adv. Sci.* **5**, doi:10.1002/advs.201800338 (2018).

16   Gur, D., Palmer, B. A., Weiner, S. & Addadi, L. Light manipulation by guanine crystals in organisms: biogenic scatterers, mirrors, multilayer reflectors and photonic crystals. *Adv. Funct. Mater.* **27**, doi:10.1002/adfm.201603514 (2017).

17   Krauss, J. *et al.* Endothelin signalling in iridophore development and stripe pattern formation of zebrafish. *Biol. Open* **3**, 503-509, doi:10.1242/bio.20148441 (2014).

18   Frohnhofer, H. G., Krauss, J., Maischein, H. M. & Nusslein-Volhard, C. Iridophores and their interactions with other chromatophores are required for stripe formation in zebrafish. *Development* **140**, 2997-3007, doi:10.1242/dev.096719 (2013).

19   Patterson, L. B. & Parichy, D. M. Interactions with iridophores and the tissue environment required for patterning melanophores and xanthophores during zebrafish adult pigment stripe formation. *PLoS Genet.* **9**, e1003561, doi:10.1371/journal.pgen.1003561 (2013).

20   Parichy, D. M. *et al.* Mutational analysis of endothelin receptor b1 (rose) during neural crest and pigment pattern development in the zebrafish Danio rerio. *Dev. Biol.* **227**, 294-306, doi:10.1006/dbio.2000.9899 (2000).

21   Patterson, L. B., Bain, E. J. & Parichy, D. M. Pigment cell interactions and differential xanthophore recruitment underlying zebrafish stripe reiteration and Danio pattern evolution. *Nat. Commun.* **5**, 5299, doi:10.1038/ncomms6299 (2014).

22   Spiewak, J. E. *et al.* Evolution of Endothelin signaling and diversification of adult pigment pattern in Danio fishes. *PLoS Genet.* **14**, e1007538, doi:10.1371/journal.pgen.1007538 (2018).

23   Volkening, A. & Sandstede, B. Iridophores as a source of robustness in zebrafish stripes and variability in Danio patterns. *Nat. Commun.* **9**, 3231, doi:10.1038/s41467-018-05629-z (2018).

24   McGuirl, M. R., Volkening, A. & Sandstede, B. Topological data analysis of zebrafish patterns. *Proc.Natl. Acad. Sci. U.S.A.* **117**, 5113-5124, doi:10.1073/pnas.1917763117 (2020).

25   Saunders, L. M. *et al.* Thyroid hormone regulates distinct paths to maturation in pigment cell lineages. *eLife* **8**, e45181 (2019).

26   Parichy, D. M., Elizondo, M. R., Mills, M. G., Gordon, T. N. & Engeszer, R. E. Normal table of postembryonic zebrafish development: staging by externally visible anatomy of the living fish. *Dev. Dyn.* **238**, 2975-3015, doi:10.1002/dvdy.22113 (2009).

27   McMenamin, S. K. *et al.* Thyroid hormone-dependent adult pigment cell lineage and pattern in zebrafish. *Science* **345**, 1358-1361, doi:10.1126/science.1256251 (2014).

28   Lewis, V. M. *et al.* Fate plasticity and reprogramming in genetically distinct populations of Danio leucophores. *Proc. Natl. Acad. Sci. U.S.A* **116**, 11806-11811, doi:10.1073/pnas.1901021116 (2019).

29   Lister, J. A., Robertson, C. P., Lepage, T., Johnson, S. L. & Raible, D. W. nacre encodes a zebrafish microphthalmia-related protein that regulates neural-crest-derived pigment cell fate. *Development* **126**, 3757-3767 (1999).

30   Zeng, Z., Johnson, S. L., Lister, J. A. & Patton, E. E. Temperature-sensitive splicing of mitfa by an intron mutation in zebrafish. *Pigment Cell Melanoma Res.* **28**, 229-232, doi:10.1111/pcmr.12336 (2014).

31   Johnson, S. L., Nguyen, A. N. & Lister, J. A. mitfa is required at multiple stages of melanocyte differentiation but not to establish the melanocyte stem cell. *Dev. Biol.* **350**, 405-413, doi:10.1016/j.ydbio.2010.12.004 (2011).

32   Zeng, H. & Sanes, J. R. Neuronal cell-type classification: challenges, opportunities and the path forward. *Nat. Rev. Neurosci.* **18**, 530-546, doi:10.1038/nrn.2017.85 (2017).

33   Gur, D., Leshem, B., Oron, D., Weiner, S. & Addadi, L. The structural basis for enhanced silver reflectance in Koi fish scale and skin. *J. Amer. Chem. Soc.* **136**, 17236-17242, doi:Doi 10.1021/Ja509340c (2014).

34   Holzinger, A., Allen, M. C. & Deheyn, D. D. Hyperspectral imaging of snow algae and green algae from aeroterrestrial habitats. *J. Photochem. Photobiol. B* **162**, 412-420, doi:10.1016/j.jphotobiol.2016.07.001 (2016).

35   Gur, D. *et al.* Guanine-based photonic crystals in fish scales form from an amorphous precursor. *Angew. Chem. Int. Ed.* **52**, 388-391, doi:DOI 10.1002/anie.201205336 (2013).

36   Dooley, C. M. *et al.* Slc45a2 and V-ATPase are regulators of melanosomal pH homeostasis in zebrafish, providing a mechanism for human pigment evolution and disease. *Pigment Cell Melanoma Res.* **26**, 205-217, doi:10.1111/pcmr.12053 (2013).

37   Lister, J. A., Lane, B. M., Nguyen, A. & Lunney, K. Embryonic expression of zebrafish MiT family genes tfe3b, tfeb, and tfec. *Dev. Dyn.* **240**, 2529-2538, doi:10.1002/dvdy.22743 (2011).

38   Gur, D. *et al.* Light-induced color change in the Sapphirinid copepods: tunable photonic crystals. *Adv. Funct. Mat.* **26**, 1393–1399, doi:10.1002/adfm.201504339 (2016).

39   Gur, D. *et al.* The mechanism of color change in the Neon Tetra fish: a light-induced tunable photonic crystal array. *Angew. Chem. Int. Edit.* **54**, 12426-12430, doi:10.1002/anie.201502268 (2015).

40   Oshima, N. & Kasai, A. Iridophores involved in generation of skin color in the zebrafish, Brachydanio rerio. *FORMA-TOKYO-* **17**, 91-101 (2002).

41   Fujii, R. The regulation of motile activity in fish chromatophores. *Pigment. Cell. Res.* **13**, 300-319 (2000).

42   Fujii, R. Cytophysiology of fish chromatophores. *Int .Rev. Cytol.* **143**, 191–255 (1993).

43   Mahalwar, P., Singh, A. P., Fadeev, A., Nusslein-Volhard, C. & Irion, U. Heterotypic interactions regulate cell shape and density during color pattern formation in zebrafish. *Biol. Open.* **5**, 1680-1690, doi:10.1242/bio.022251 (2016).

44   Engeszer, R. E., Wang, G., Ryan, M. J. & Parichy, D. M. Sex-specific perceptual spaces for a vertebrate basal social aggregative behavior. *Proceedings of the National Academy of Sciences of the United States of America* **105**, 929-933, doi:10.1073/pnas.0708778105 (2008).

45   Eom, D. S., Bain, E. J., Patterson, L. B., Grout, M. E. & Parichy, D. M. Long-distance communication by specialized cellular projections during pigment pattern development and evolution. *Elife* **4**, doi:10.7554/eLife.12401 (2015).
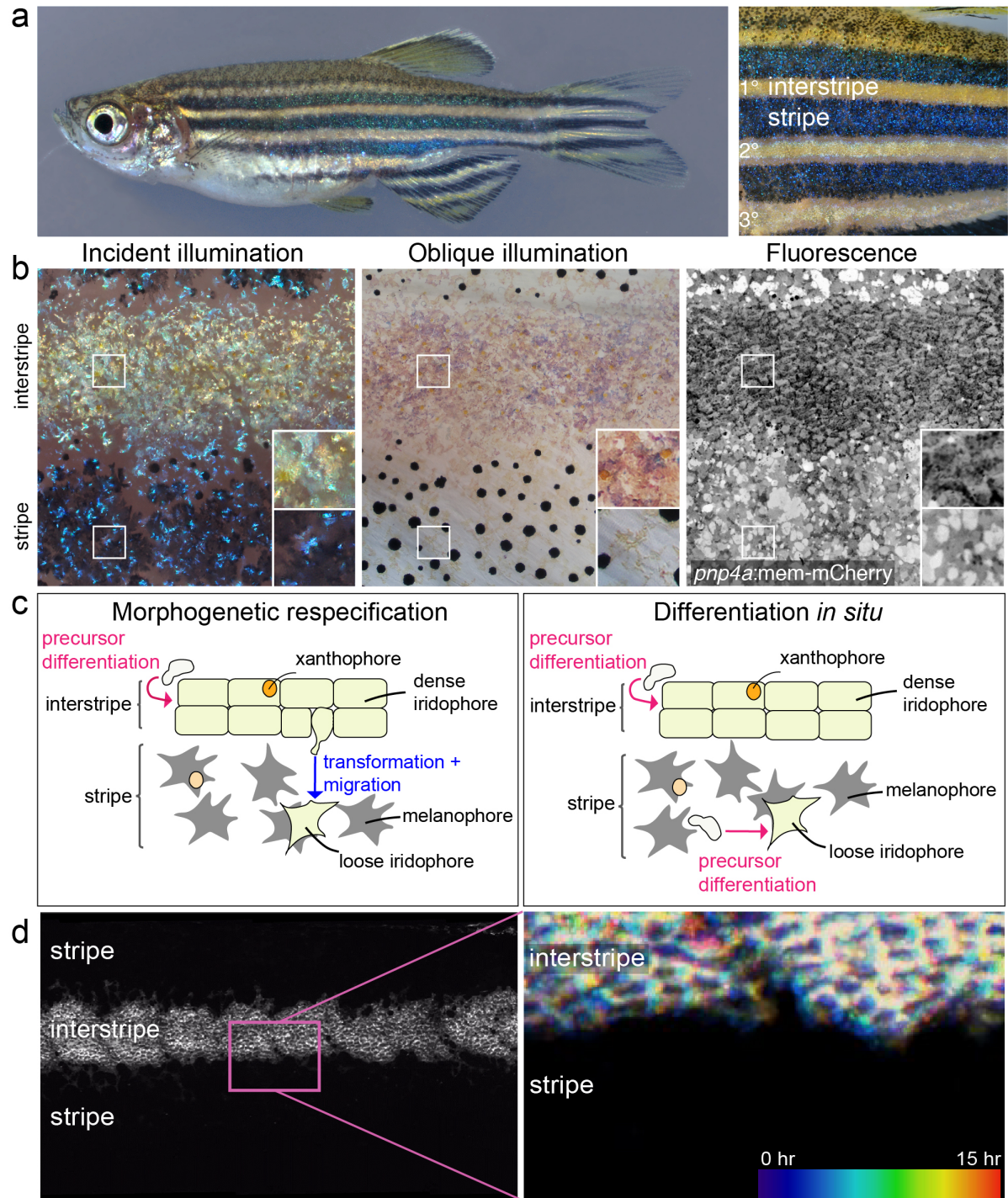
1
2 **Figure 1. Anatomy, development and models of zebrafish adult pigment**
3 **patterning. (a)** Left panel, an adult zebrafish showing light interstripes with intervening
4 dark stripes. Right panel, a closeup showing the primary interstripe (1°) which develops
5 first with stripes above and below, followed by secondary interstripes ventrally (2°) and
6 dorsally with additional stripes, and ultimately a tertiary (3°) interstripe and stripe. **(b)**
7 Closeups of first-forming (primary) interstripe and stripes, illustrating overall pattern
8 features as well as morphologies and arrangements of iridophores. All panels are the

1   same location in a single animal. Left panel is incident illumination showing iridescence
2   of iridophore-reflecting platelets with yellowish tinge in the interstripe and bluish tinge in
3   the stripe. Center panel is oblique illumination revealing surface features and non-
4   iridescent colors of iridophores. Right panel is membrane-targeted mCherry (mem-
5   mCherry) driven at high levels in iridophores by regulatory elements of *purine nucleoside*
6   *phosphorylase 4a* (*pnp4a*) (Eom et al., 2015[45]; Saunders et al., 2019[25]; Spiewak et al.,
7   2018[22]) to reveal cell boundaries and arrangements. Pixel values are inverted for easier
8   comparison to brightfield images. **(c)** Two models for iridophore patterning in interstripes
9   and stripes. In the morphogenetic respecification model (left panel), initially densely-
10   packed, cuboidal iridophores begin adopting a loose morphology as they and their
11   progeny migrate out to populate the prospective stripe. In the differentiation *in situ* model
12   (right panel), iridophores residing in interstripes and stripes are different cell types that
13   have differentiated 'in place' from a precursor population. Hence, loose iridophores in
14   stripes are not lineally related to dense iridophores in interstripes. **(d)** The flank of a 7.5
15   standardized standard length (SSL) *pnp4a*: mem-mCherry fish. Left panel; fluorescence
16   image showing the arrangement of labeled cells in the dense primary interstripe. Right
17   panel; pseudo-temporal coloring representation of a 15 hour time-lapse movie (zoomed
18   to the region outlined in 'd') revealing that interstripe iridophores migrate primarily in the
19   anteroposterior direction, with no apparent dorsoventral migration into the stripe region.
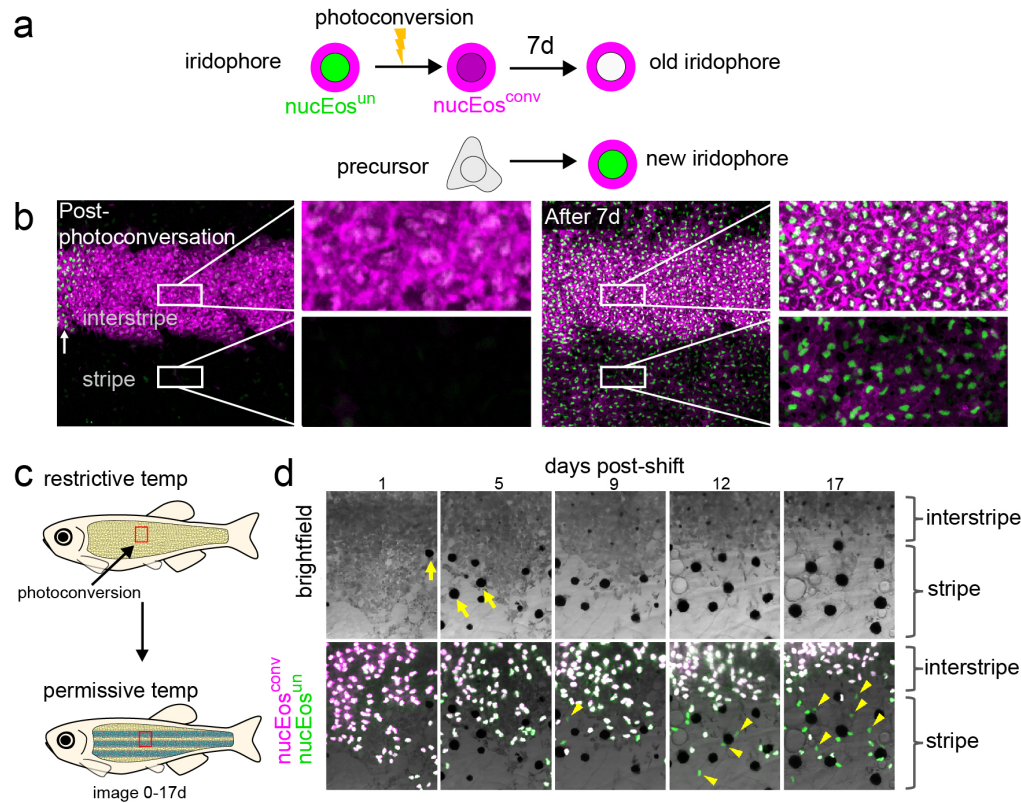20
21
22
23
24

1
2
3 **Figure 2. Photoconversion experiments to test models of pattern development and**
4 **remodeling. (a)** Fish were created that have iridophores expressing nuclear localizing
5 Eos (nucEos^{un}, green) and a membrane-targeted mCherry (mem-Cherry, magenta)
6 driven by regulatory elements of *pnp4a*. Following photoconversion of an iridophore
7 population, the converted nuclei will appear magenta (nucEos^{con}). After 7 days,
8 previously photoconverted nuclei will appear white (due to the combination of 'new'
9 green proteins and 'old' magenta proteins), whereas nuclei of newly differentiated cells
10 will appear green. **(b)** Tracking photoconverted iridophores in the interstripe revealed
11 stripe iridophores do not derive from the interstripe population. Following
12 photoconversion of a region in the primary interstripe of a fish at 7.5 SSL, all nuclei
13 appeared magenta (Post-photoconversion), with surrounding mem-Cherry labeled
14 plasma membrane magenta-colored as well (left panel). After seven days of additional
15 development (8.6 SSL), at which time iridophores now populate the primary stripe, only
16 nuclei with green signal are seen in the stripe zone, whereas interstripe nuclei are
17 primarily white (right panel). In zoom-up images, interstripe iridophores are seen to have
18 continued to proliferate and retained nucEos^{conv}, acquiring new nucEos^{un} (making their
19 nuclei white) (upper inset, right panel). Stripe iridophores, by contrast, lacked nucEos^{conv}
20 and expressed only nucEos^{un} (making their nuclei green) (lower inset, right panel). **(c)**
21 Use of a temperature-sensitive *mitfa^{vc7}* fish to examine the effect of conditional
22 melanophore development on iridophore pattern remodeling. In this experimental setup,
23 iridophores were labeled only with a nuclear-localizing Eos (nucEos^{un}, green), so that
24 following photoconversion their converted nuclei would appear magenta (nucEos^{con}). **(d)**

17

1   Brightfield (upper) and fluorescence superimposed on brightfield (lower) following

2   photoconversion and shift to permissive temperature to drive onset of melanophore

3   differentiation. Iridophores labeled by nucEos expression were photoconverted at the

4   beginning of the experiment and followed over 17 days to distinguish newly

5   differentiating iridophores (green nuclei) from previously differentiated iridophores

6   (white). As melanophores differentiated (see yellow arrows in top panel), the region of

7   dense morphology iridophores receded dorsally. This change was accompanied by

8   differentiation of new iridophores having green nuclei (see yellow arrowheads in bottom
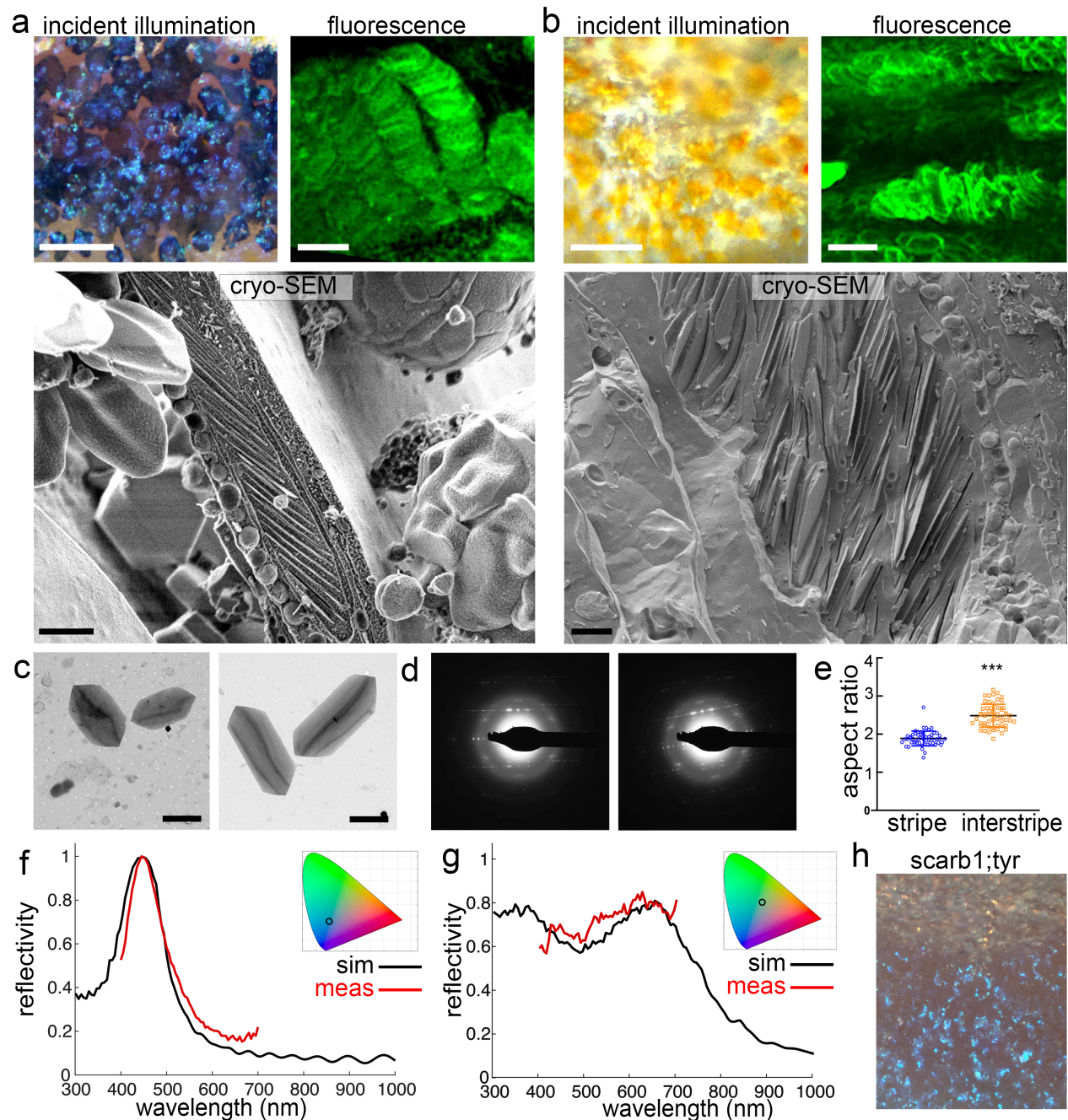
9   panel) in the newly forming stripe.

10

11

1

Figure 3. Loose- versus dense- iridophores have distinct crystal morphologies
and ultrastructural organizations but shared chemistry. (a) Loose iridophores in
stripe region viewed by incident illumination, fluorescence and high pressure–frozen,
freeze-fractured cryo-SEM (Cryo-SEM). The incident illumination image shows blue
iridophores on top of black melanophores; the fluorescent image reveals malachite
green (MG) labeled iridophores with highly ordered arrays of guanine crystals; and the
Cryo-SEM image shows iridophore cytoplasm with highly disordered arrays of crystals.
(b) Dense iridophores in interstripe region viewed by incident illumination, fluorescence
and Cryo-SEM. The incident illumination image shows silvery iridophores covered by
yellow xanthophores; the fluorescent image reveals MG labeled iridophores with

1   disordered arrays of guanine crystals; and the high pressure–frozen, freeze-fractured
2   cryo-SEM micrograph shows iridophore cytoplasm with disordered arrangements of
3   crystals. **(c-e)** TEM analysis of crystals isolated from iridophores from either the stripe or
4   the interstripe regions. (c), TEM micrographs of crystals isolated from stripe (left panel)
5   and interstripe regions (right panel); (d), TEM-based electron diffraction of crystals
6   isolated from stripe iridophores (left panel) and interstripe iridophores (right panel); (e)
7   graph of aspect ratio (length/width) of stripe iridophores (blue) and interstripe iridophores
8   (orange), *p*<0.0001. **(f)** Simulated reflection (black) and measured reflection (red) from a
9   stripe iridophore. **(g)** Simulated reflection (black) and measured reflection (red) from an
10   interstripe iridophore. Insets in both (f) and (g) show the corresponding reflectance color
11   on a CIE (International Commission on Illumination) chromaticity space diagram. **(h)**
12   Incident illumination image of an adult fish lacking melanin in melanophores and
13   carotenoids in xanthophores due to mutations in *tyrosinase* and *scarb1*, respectively.
14   The image shows iridophore-type specific coloration is independent of melanin and
15   carotenoids, consistent with reflectance data obtained for stripe (f) and interstipe
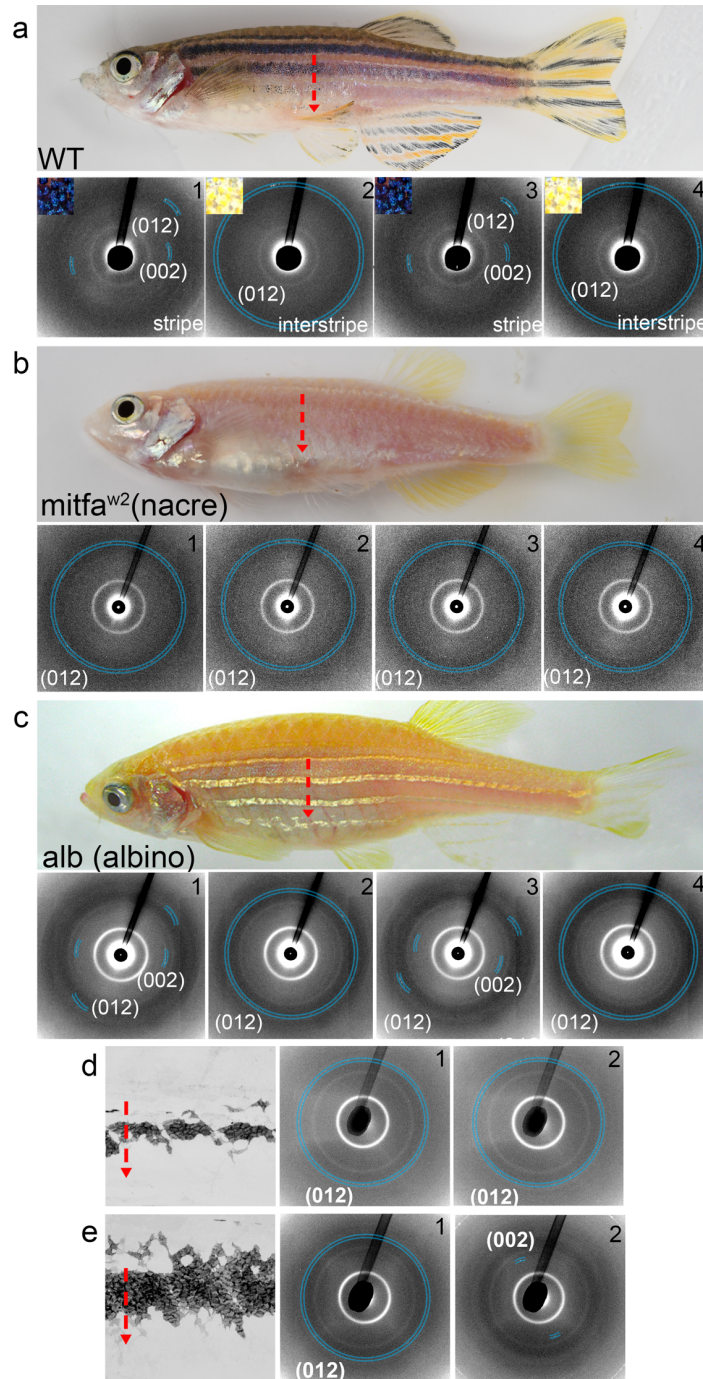16   iridophores (g).

20

1
2
3 **Figure 4. Disordered- and ordered- crystal-containing iridophores remain distinct**
4 **throughout development. (a)** Upper panel shows wildtype zebrafish with the red
5 vertical dotted arrow showing where X-ray diffraction measurements were made. Lower
6 panels 1 through 4 show X-ray diffraction pattern measurements in stripe and interstripe
7 regions, with upper left insets showing the incident illumination differences in these
8 regions. Diffraction patterns collected in the stripe regions (1 and 3) had low angular
9 distributions with a punctuated-like signal, indicating iridophore crystals in these regions

1   are parallel to one another. Diffraction patterns collected in the interstripe regions (2 and
2   4), by contrast, exhibited high angular distributions with a full-ring signal, indicating
3   iridophore crystals in these regions are not well aligned. **(b)** X-ray diffraction
4   measurements as in (a) made in Mitfa-w2 mutant (nacre) fish using a vertical line scan
5   across the trunk of the fish. The typical diffraction pattern of the ordered stripe iridophore
6   is missing in this line scan, and the observed diffractions are of high angular distribution
7   ("full ring). **(c)** X-ray diffraction measurements as in (a) made *albino* mutant (*alb*). The
8   overall diffraction pattern resembles that of wild type fish, with highly ordered diffraction
9   patterns of the (002) and (012) diffraction planes throughout the stripe region (1 and 3),
10   and high angular distribution of only the (012) diffraction plane throughout the interstripe
11   region (2 and 4). **(d)** X-ray diffraction patterns from a vertical line measured across the
12   trunk of a ~6 SSL wild-type zebrafish. Panels 1 and 2 show X-ray diffraction patterns
13   from areas in the 1° interstipe and adjacent to the 1° interstipe, respectively. Both
14   patterns show a high angular distribution of the (012) diffraction plane. (**e**) X-ray
15   diffraction patterns from a vertical line measured across the trunk of a ~6.9 SSL wild-
16   type zebrafish. Panels 1 and 2 show X-ray diffraction patterns from areas in the 1°
17   interstipe and adjacent to the 1° interstiperespectively. A low angular distribution
18   diffraction of the (002) plane (2) is visible just adjacent to the first interstripe region (1).
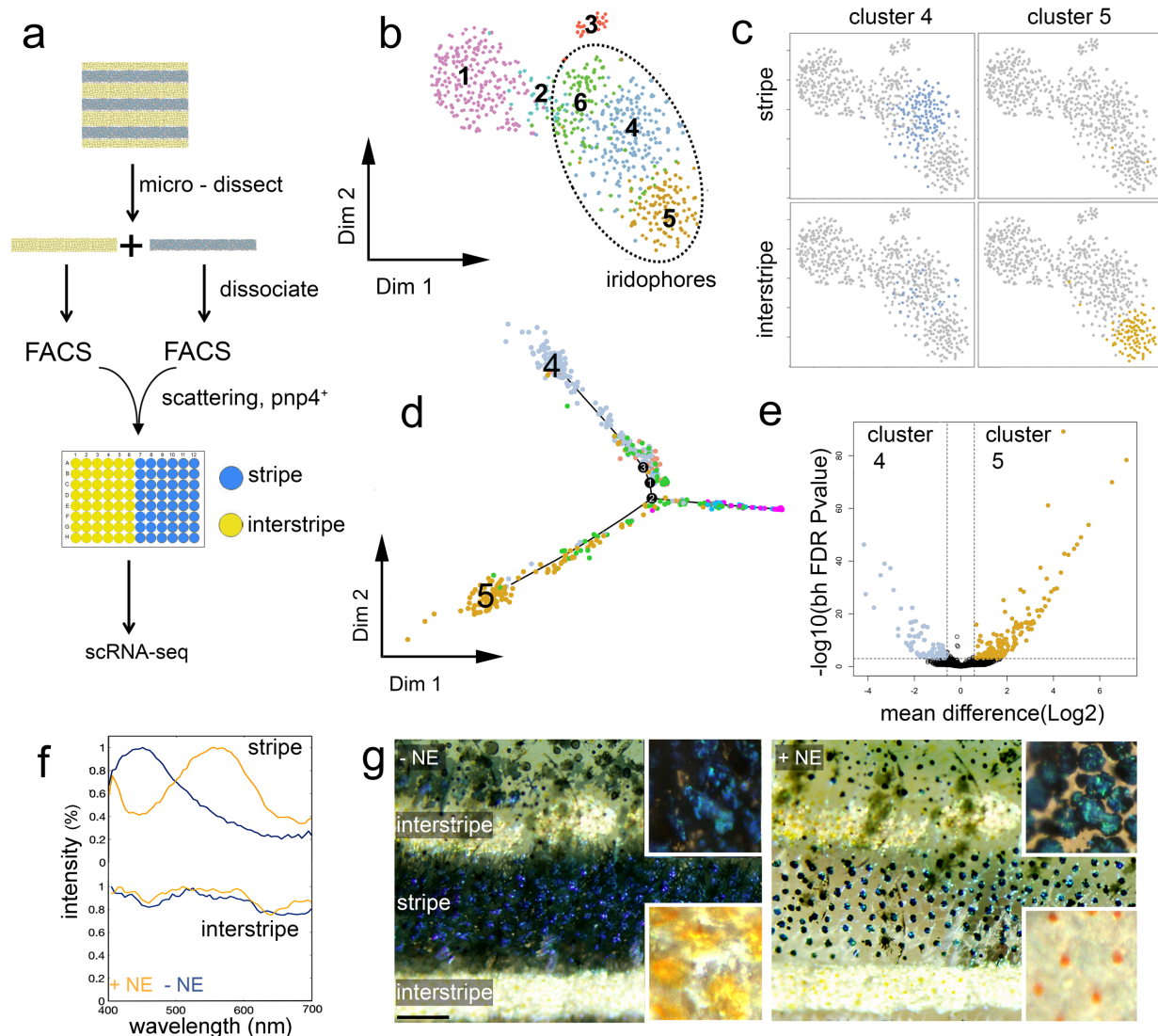19
20
21

22

1

2 **Figure 5. Disordered- and ordered- crystal-containing iridophores exhibit distinct**
3 **transcriptomic signatures and response to stimuli. (a)** Experimental design of single
4 cell RNA sequencing experiment. **(b)** Two-dimensional tSNE representation of the
5 collected skin cell clusters (dashed ellipse marks iridophores). **(c)** Anatomical origin of
6 iridophores clusters. **(d)** Pseudo-time trajectory of the collected skin cells. **(e)** A volcano
7 representation of differentially expressed genes between clusters 4 (light blue) and 5
8 (orange). **(f-g)** The response of an adult zebrafish skin pattern to norepinephrine (NE)
9 stimuli. (f) is the optical response of individual iridophores from the stripe (upper panel)
10 and interstripe (lower panel). In the stripe, the reflection peak of an ordered iridophore
11 shifts from ~450 nm to ~570 nm upon NE treatment. In the interstripe, only minor
12 changes in the reflection spectra occur in response to NE. (g) is the optical response of
13 the relaxed, untreated fish (-NE) compared to the treated fish (+NE). Note the contrast
14 between the blue stripe and the two-flanking yellow interstripes and how this changed
15 with NE treatment. Before treatment, a deep blue color for the stripe region and a
16 golden-yellow color for the interstripe region is observed. After NE treatment, the

1 contrast between the stripe and the interstripe is drastically reduced. This color change
2 arises because NE causes melanophores in the stripe to aggregate and blue iridophore
3 reflectance to shift from a dark-blue to green-yellow hue (see upper insets), while in the
4 interstripe, NE causes xanthophores to aggregate and silvery iridophores to have only a
5 minor color change (lower insets).
6
7
8